Design, development, and testing of a hybrid *in situ* testing device for building joint sealant

C. White,[a] N. Embree, and C. Buch
Building and Fire Research Laboratory, National Institute of Standards and Technology, Gaithersburg, Maryland 20899

R. S. Williams
USDA Forest Service, Forest Products Laboratory, Madison, Wisconsin

(Received 31 March 2004; accepted 17 January 2005; published online 1 April 2005)

The testing of sealant samples has been restricted to devices that either focus on fatiguing multiple samples or quantifying the mechanical properties of a single sample. This manuscript describes a device that combines these two instrumental designs: the ability to both fatigue and characterize multiple sealant samples at the same time. This device employs precise movement capability combined with a stiff loading frame and accurate force measurement for the characterization of five ASTM C719 sealant samples. The performance of this device is demonstrated by monitoring the changes in mechanical properties of silicone sealant during the first 90 h of cure. A complete description of the apparatus, results from the study of curing and analysis is included. [DOI: 10.1063/1.1889234]

INTRODUCTION

Modern design relies heavily on sealant materials to provide waterproofing and moisture barrier protection to the building and its components. Nearly 60% percent of "gun grade" sealant produced globally is currently used in construction, creating a $30 billion per year industry.[1] In 1996, this was 420 000 000 kg of material that could be spread over 58×10^6 km of joints.[2]

Despite the central role sealants play in maximizing building envelope performance, they receive little attention from the end user leading to premature joint failure. Results from recent studies in England predict that 55% of installed sealant joints will fail within 10 years of installation and 95% of all sealant joints will fail within 20 years.[3] This information is consistent with previous studies from Japan[4] and Germany,[5] but is in contrast with implied manufactures warranties of (35–50) years or even the lifetime of the building.

Additionally, the premature failure of sealant significantly contributes to the second most commonly cited complaint in the annual National Association of Home Builders homeowner surveys, that of water leakage into a home.[6] To repair and maintain American homes, the US Census Construction Report consistently shows homeowners spending (65–70) billion dollars per year.[7] Much of this is believed to be due to water leakage.

A critical factor in the inappropriate selection of sealant formulations has been the reliance on data from threshold type tests like ASTM C719. These tests are qualitative and have little predictive capability because they have little correspondence to the actual in-service environment. For example, ASTM C719 establishes the performance of the sealant through the following protocol: a one month period of static cure, followed by sequential stress regime including immersion in water (7 d), baking in an oven (7 d), exposure to UV, and finally mechanical cycling.[8] The samples are then visually evaluated for defects.

This article describes efforts to design, produce, and test a hybrid device allowing for sealant sample deformation, which concurrently fatigues the sample (sealant community) and characterizes the mechanical properties (polymer science community) of the sealant. In addition, this device features multisample, multicycle, automation and informatics capabilities that enhance the characteristics of traditional sealant testing devices. The performance of this instrument is demonstrated by monitoring the change in a silicone sealant during the initial hours of curing. Finally, this experimentally monitored change in mechanical properties is linked to a molecular model of the changes occurring during the cure of the sealant. This device is the first generation of a class of sealant instruments that will provide the experimental data required to significantly improve the predictive capability of current sealant testing and evaluation methodologies. The first task in developing a device to monitor changes in sealant is to understand the polymer science related to sealant formulations.

POLYMER SCIENCE

Sealant formulations are polymer systems that increase in molecular weight during the cure period by one of several mechanisms,[9] The most prevalent of which is crosslinking. Understanding, quantifying, and predicting crosslink formation has received intense interest from the polymer science community for the past 50 years. A selection of the relevant literature is cited here.[10–20]

[a]Author to whom correspondence should be addressed; electronic mail: christopher.white@nist.gov

In polymer science, several techniques are used to monitor changes in the crosslink density commonly or the molecular weight between crosslinks or M_c of polymer systems. The three most prelevant are: measuring changes in T_g, measured with differential scanning calorimetry; swelling with a solvent measured either by dimensional changes or weight gain; or by measuring the modulus of the rubbery plateau. Of these, the method that offers the most promise as an *in situ* monitor of the sealant properties is measuring the modulus of the rubbery plateau.

This is a common method for a two reasons: one, the readily available precision of both stress and strain measurements, and two, the direct linkage between these macroscopically measured quantities and a well documented fundamental description of the molecular mechanism. This direct linkage between the stress and strain and the molecular mechanism is well established for neat polymer systems. It is less well established for filled systems such as sealant, but this is a good first approximation. The M_c can be calculated from the initial response of the sealant joint to tensile stress by the following equation.[9]

$$\frac{3}{5}\sigma = \frac{\rho}{3M_C}RT\left(\alpha - \frac{1}{a^2}\right), \tag{1}$$

where σ (engineering stress)=force/area; ρ is the density of the sealant; R is the gas constant; T is the temperature in K; and α is the extension ratio ($\alpha = L/L_o$, where L_o is the original length and L is the deformed length). Equation (1) includes two modifications proposed by Payne[21] and Gent.[22] These two corrections accounts for (1) the differences between the Young's modulus and the apparent modulus for a sample with constrains with arising from the geometry typically used in sealant testing (described in the experimental section) and (2) the large deformation of the sample. The correction for the constrained geometry is evident by the $3/5$ factor in front of the engineering stress, while the finite extension correction is evident by the $(1/3)(\alpha - 1/\alpha^2)$ in the right side of the equation. Further finite element studies by Ketcham *et al.*[23] have indicated that these two corrections for the constrained geometry and large extension may be as much as 20%–30% high, but still involves a vertical shift to the stress measurement. The need for these corrections will be present in any instrumental design.

Measurements of the modulus in the rubbery plateau are usually made with single sample devices. Both the force and deformation measurements are well defined and precisely quantified. The samples are usually formed into a specific geometry. Commercial mechanical testing devices are often used in this type of testing; for example, Instron markets such a device.[24] Typically, these tests are conducted at much higher speeds (50 mm/min) than those performed in the sealant community (0.06 mm/min), so as to minimize the time consumed of an expensive physical testing device.

MOTIVATION FOR A HYBRID DEVICE

To significantly improve the predictive capability of current sealant testing methodologies, predictive models of behavior must be developed and experimentally verified. Obtaining the required experimental data using traditional means from either the polymer science or sealant community is not feasible due to two factors: the destructive nature of the tests and the labor required to measure each sample. Currently, studies of sealant durability that incorporate movement involve using simply constructed, multisample devices (e.g., mechanical vices).[25] Even in the most ambitious studies, it is only at the end of the exposure period that the mechanical properties of the sealant samples are destructively evaluated using the analytical instrumentation described above. The standard testing protocol for most studies leads one to make conclusions about sealant failure solely on visual observation of the material.

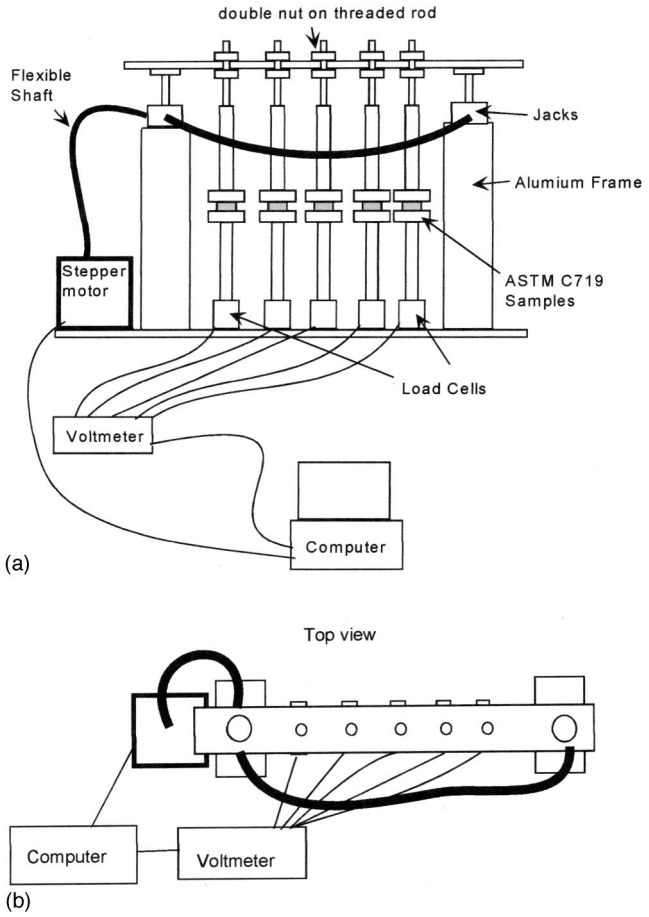

FIG. 1. A line drawing of the side view (a) and top view (b) of the hybrid sealant testing device. Note that the load cells are located on the fixed side of the frame.

DESIGN REQUIREMENTS

Several functional requirements were important in the design and construction of this device including characterization of the rheological properties of the samples requiring high-precision movement and forces measurement capabilities, accommodation of multiple samples, automated operation, and low cost. Since this device will generate an independent data file for every cycle and for every sample, an informatics system to handle the data is required.

A critical consideration was the number of samples to be cycled. To increase the confidence in the data, a large num-

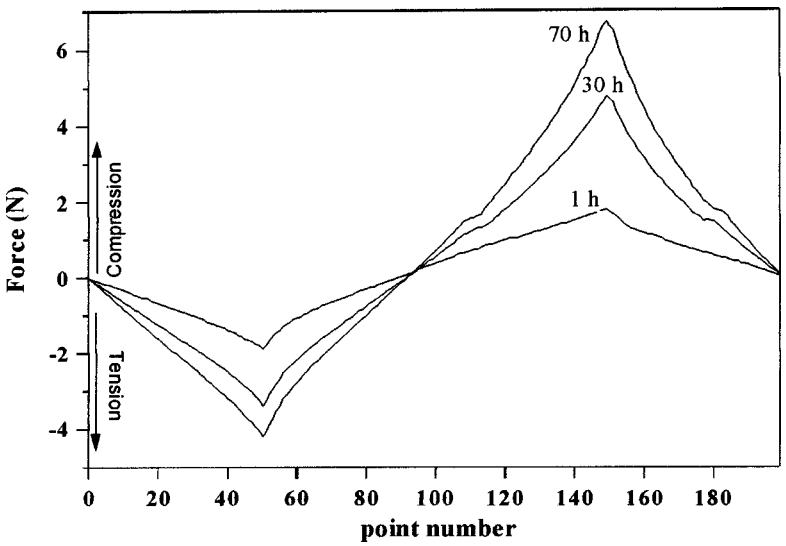

FIG. 2. Plot of the force recorded from the load cell of one of the samples as a function of deformation cycle number. The lines represent a smooth line drawn between the 200 data points for each deformation cycle. The data from four deformation cycles are plotted: 1, 30, 70, and 90 cycles. The end play in the screw is clearly evident in the one-cycle data.

ber of samples are required. Large sample sizes significantly increase the total force required for the machine since the total force is equal to the maximum force required to deform one sample multiplied by the total number of samples. The balance between these considerations resulted in five ASTM C719 sized samples as the number and type included in this design. The consensus of a group of key sealant industry researchers was that 90 kg would be sufficient to fail any sealant sample in any configuration. Therefore, the design frame and movement system must handle 450 kg of force.

High-precision movement is required to characterize the samples. Sealant studies involve between 7.5% to 100% relative joint movement of a standard 1.27 cm sealant joints. An acceptable upper limit of 10% for the relative standard uncertainty in the determination of modulus (which is calculated by the stress/strain) was discussed with members of our industry consortium for this device. This leads to a requirement that the displacement be controlled to at least ±0.05 mm. The stress measurement requires less consideration due to the availability of high-precision cost-efficient load-measuring devices.

IMPLEMENTATION OF THE DESIGN REQUIREMENTS

Load frame

Several single-arm designs were considered, prototyped, and rejected because of excess compliance: >0.05 mm. The final design, depicted in Fig. 1, is similar to commercial instruments designed to characterize the mechanical properties of samples. In this design, a stiff U-shaped frame limits movements in any but the vertical direction. The frame is constructed from $8\ \text{cm}\times 10\ \text{cm}\times 50\ \text{cm}$ solid aluminum blocks connected to $8\ \text{cm}\times 50\ \text{cm}$ I-channel aluminum crosspieces on the top and bottom. This frame showed no detectible deflection (measured with ±0.01 mm precision) with a load of 450 kg placed in the center of the span when stressed in both tension and compression.

Sample attachment

The samples are attached to this frame by 1.9 cm aluminum rods extending from the top and bottom of the frame. The aluminum sample supports are tapped and threaded $(\frac{1}{4}, 28$—this specifies the screw size and thread). The lower 1.9 cm rod is taped and connected to the load cell by a threaded $(\frac{1}{4}, 28)$ stud; the load cell is bolted into the lower frame. The upper end of this lower rod is taped $(\frac{1}{4}, 28)$ and a threaded stud connects to the sample. The upper 1.9 cm rod connects to the sample in an analogous method to the lower support rod. The upper end of the upper rod is taped for a larger stud $(\frac{1}{4}, 13)$. This stud easily passes through a hole in the upper frame and turns with little resistance. Once the samples have been loaded, this stud is secured in place by tightening nuts $(\frac{1}{2}, 13)$ on either side of the upper frame.

A sample is attached by spinning it onto the threaded stud of the fixed lower rod. This procedure is followed by spinning the upper rod and attached stud to engage the threads on the aluminum sample support. When the upper and lower rods are secured to the sample, the upper rod is then secured to the frame by tightening the nuts $(\frac{1}{2}, 13)$ below and above the upper frame crossbar.

Displacement control

For the displacement control, there are four sources of uncertainty in this system: the precision of the vertical displacement of the frame (jacks), the precision of the motor displacement, the coupling of the motor to the jacks, and the compliance of the frame. Each of these systems is discussed below. The total displacement uncertainty of the system is then measured and compared with each of these potential sources of uncertainty.

Synchronized precision twin screws, one on each side of the heavy aluminum I-channel top crossbar, provide precise one-dimensional cyclic motion control. Additional motion stability was provided by including 1 cm aluminum guide rods, mounted on each side of the frame and bearings mounted on the top I-channel crosspiece.

To provide fine control of the vertical motion of the upper I-channel crosspiece, precision screw jacks obtained from Joyce Corporation[24] (WJ1000) were mounted on top of $8\ \text{cm}\times 8\ \text{cm}$ aluminum block and connected to the upper I-channel. Each of these precision Joyce Jacks (WJ1000) has

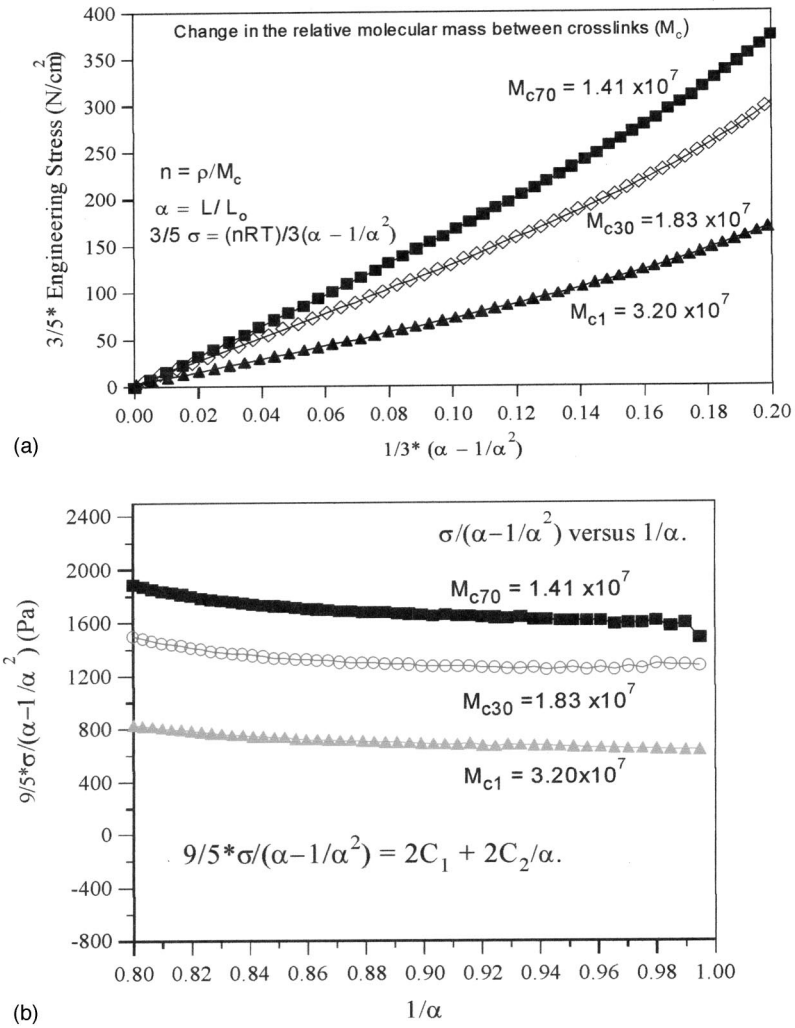

FIG. 3. The calculation of the molecular weight between crosslinks (M_c) is shown in (a) for the four deformation cycles depicted in Fig. 2. For data plotted in this way, M_c, is inversely proportional to the slope of the curve. (b) The same data plotted in a Mooney-Rivlin format to check for the applicability of the neohookean model. Since the plot shows little evidence of a dependence on $1/\alpha$, the use of the neohookean model is appropriate.

a fine thread resolution of 0.64 mm/revolution with a lead screw uncertainty of ±250 nm/mm of vertical travel. When converting from tension to compression, there is 0.2 mm±0.05 mm of endplay in the jack threads. To minimize any impact this might have on the measured force response curve, the force measured during the first 0.2 mm of displacement upon reversal is recorded but not used in the determination of the force response curves discussed later. The screw torque is the force required to keep the screw from rotating is specified to be 3.0 N m. The running torque at 8.33 revolutions per second (rps) is 1.1 N m.

Coupling the jacks to each other and to the motor is accomplished through the use of flexible shafting. A future version of this device will operate in tight spaces. Flexible shafting was selected because it allows the unit to be more compactly designed than if traditional stiff shafting was selected. The flexible shafting was obtained from S.S. White Inc. (model number 375M).[24] With this shafting, the torque capacity is a function of the bending radius of the shaft. With a bend of greater than or equal to 20.3 cm radius, this shaft could supply 6.1 N m of torque.

The last component to be specified was the motor supplying the torque. A stepper motor system was selected for two reasons: the ease of automation and the high degree of precision in the movement. Typically, stepper motors provide 25 000 steps/revolution, which is equivalent to a nominal vertical resolution of ±25 nm. The Compumotor Zeta Series® 6104 with a TS42B motor selected for this design delivers 17.61 N m of static torque with a running torque (at 8.33 rps) of 4.2 N m when wired in series. It has more than enough torque to accommodate the maximum expected static torque of 3.1 N m and running torque at 8.33 (rps) of 1.1 N m. The torque/load curve of this motor sets the upper limit of the speed of this device. The 8.33 rps quoted above corresponds to 317 mm/min, which is much larger than the 50 mm/min that is typical for a standard polymer science testing speed. This upper limit of 317 mm/min at maximum load conditions gives this device the ability to function like a multisample traditional testing device in addition to the more conventional operation.

The compliance of the entire device was measured by replacing the center sealant sample with a block of steel machined to ASTM C719 sample dimensions. The resulting force displacement curve is then used to derive the compliance for the device, which is ±0.005 mm/kg of force. The standard tests for sealants require a movement of ±3 mm (25% of a ASTM C719 sample configuration). In discussions with members of the sealant industry, it is commonly assumed that no force greater than 10 kg has been observed for a 25% expansion of a sealant in an ASTM C719 configura-

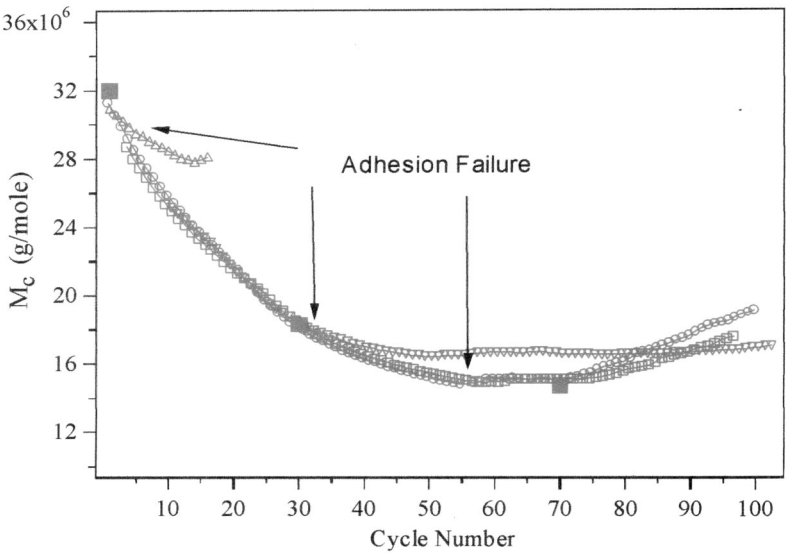

FIG. 4. The calculated values for M_c for each of the five sealant samples. The calculated values from Fig. 3 are depicted as solid circles on this figure. The initial decrease is due to increasing cure or crosslink density, while the increase is believed to be caused by adhesive failure of the samples.

tion. This results in a worst-case standard uncertainty in of ±0.05 mm in a 25% expansion of the sealant of 3 mm or 1.5% relative standard displacement uncertainty.

This 1.5% relative standard uncertainty is the combination of the four previously discussed sources: motor precision, coupling of the motor to the jacks, the jacks themselves, and the compliance of the load frame.

Load Measurement

To measure the force required for movement, each of the five samples had an Interface load cell (SM-250) bolted to the lower frame as depicted in Fig. 1. The load cell was wired to its matched and jointly calibrated Interface SGA conditioner/amplifier. The load cell and SGA conditioner/amplifier were calibrated by Interface prior to arrival at NIST. The output from conditioner/amplifier was calibrated so the linear range of −10 to 10 V output corresponds to −91 to 91 kg with a manufacture's reported nonlinearity of <0.02%. To measure all five of the voltage signals, a Keithley 2700 multimeter with a 20 channel, 22 bit A-D resolution multiplexer card option, model #7700, is used. The multimeter is configured to scan and measure the voltage on each channel and report that information to the computer through the GPIB interface. The multimeter will report the voltage with a stated precision of 6.5 digits. For a 10 V signal, this would correspond to <0.001% or much less than the stated nonlinearity of the load cell (<0.02%). Thus, the relative standard uncertainty on the load signal is estimated at ±0.02% primarily due to the nonlinearity of the load cell.

TOTAL MEASUREMENT UNCERTAINTY

The measurement that is of interest is the slope of the stress over the strain. By summing the relative standard uncertainty of the motional displacement (1.5%) and the relative standard uncertainty on the load signal is estimated at ±0.02% an estimate of approximately 1.6% in relative standard uncertainty in the measurement of the engineering modulus. The initial acceptable limit of 10% relative standard uncertainty has been well exceeded.

Automation

A computer running a custom LABVIEW® program controls the movement and force monitoring of the system. The program sends a signal to the motor resulting in the vertical motion described above. At the end of that vertical motion, the multimeter is instructed to measure the voltage on each of the five channels. This voltage, or force measurement signal, is then sorted and stored in an array, downloaded to the computer, and stored in a separate file for each channel. This entire process is repeated for each point in the deformation profile. The 200 equal distance point deformation profile consists of 50 points of expansion, 100 points of compression, and 50 points of expansion to return to the original starting position. Changes in the speed or extent of sample motion are accomplished by changing the velocity of the stepper motor or the number of steps executed to acquire a data point. This approach has two principle advantages. First, it creates a uniform format for the output data files and second, allows the motor driver/indexer to produce smooth motion for each data point. Once a deformation cycle has been completed, the program loops back to begin the process of deforming the samples again repeating this process until either the program is terminated or the prescribed number of cycles has been completed. A typical deformation cycle takes ~1 h to complete.

Informatics

Test data are stored in two locations: on the computer connected to the instrument and in a large database on a remote server. Because of the volume of data that is generated (~3000 files/month), it is necessary to develop a secondary storage method to catalog the data. The main functions of the informatics system are to store, sort, search, and retrieve data files. The system automatically creates a record for each deformation file on a remote dedicated server-computer connected through an ethernet connection. This record system contains fields to identify each data file such as operational time, date of acquisition, material, substrate, experimenter, experiment name, etc. It also maintains the

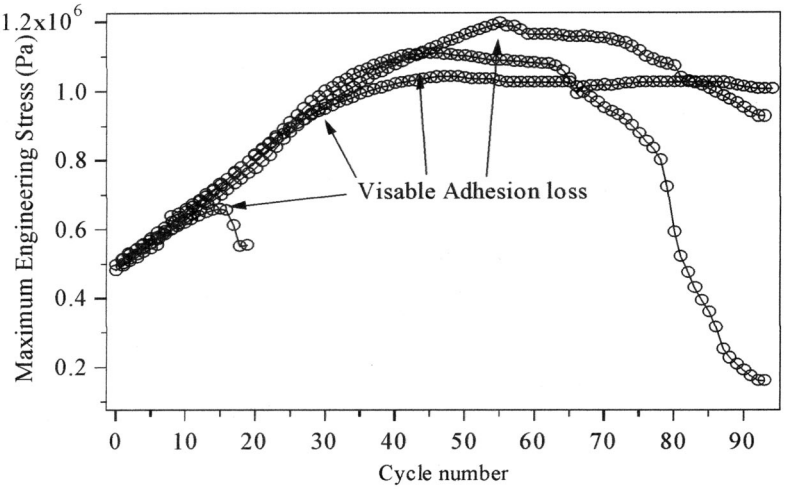

FIG. 5. The maximum tensile stress recorded during a deformation cycle is plotted as a function of cycle number. Four of the samples show a similar increase in tensile force up to 40 cycles with a fifth showing early changes in maximum tensile stress, attributable to adhesive failure. All of the other samples show a drop in the maximum tensile stress attributed to adhesion failure.

name of the file where the specific raw data values are stored. Raw data are not included within the database. This method is commonly called a meta-data database. A meta-data database method was selected based upon its ease of development and inherent flexibility in the types of data that can be stored. Once the automated process creates the records in the meta-database, data files are automatically renamed according to the metadata records and uploaded to the remote database server using a visual basic script.

A series of active server pages (.*ASP) allow queries of the remote server query language server through the use of standard browser software. These pages allow a user to select and sort the data of interest, select the files to be downloaded, and download these files to any location on the browsers' computer (the downloading requires the use of a javascript applet from Informentum, LTD).

The previous sections have described the instrumental development in great detail. In the next sections, the performance of the instrument will be demonstrated by monitoring a sealant during cure.

EXPERIMENT

The mechanical properties of a sealant undergo the greatest change during curing. Thus, this is an ideal time to evaluate the range of performance of this hybrid device. A major sealant producer provided a model commercial silicon sealant formulation used in this study. It was gunned into a 5.08 cm $\times$ 1.27 cm $\times$ 1.27 cm sample cavity composed of 7.62 cm $\times$ 1.27 cm $\times$ 1.27 cm aluminum supports on each side with a polytetrafluoroethylene (PTFE) film on the bottom and 1.27 cm $\times$ 1.27 cm PTFE spacers on each end. This is a typical ASTM C719 sample size. The samples were cured in this fixture for 4 h and then removed, keeping the PTFE spacers and the aluminum substrates intact. After another 4 h of cure, the samples were threaded onto the sealant tester using the procedure described above and the end cap spacers were removed.

A feature of this instrument is that any arbitrary displacement wave form can be imposed on the sample. This flexibility can be used to provide more extensive characterization of the mechanical properties in future studies. For this study, a simple tension and compression deformation cycle was selected with a movement of ±25% of the 1.27 cm joint width or 3.18 mm ± 0.05 mm deformation in each of the positive and negative direction. The deformation cycle was divided up into 0.254 mm steps or data points. After each step was completed, the load was measured on each of the five load cells using the above-described system. The velocity of the motor was 0.254 mm/min with a 15 s total step time to collect the load cell data. This gives a nominal rate of movement of 0.212 mm/min. This results in a 56 min cycle time. This rate is higher than that typically used in ASTM C719 testing, but within the range used to evaluate sealants.[26]

RESULTS

Typical results from a deformation cycle are shown in Fig. 2. In this figure, the 200 points that compromise the data cycle are plotted along the x axis and the voltage from a load cell is plotted on the y axis. The results from cycle numbers 1, 30, and 70 are plotted on this figure.

The ability to quantitatively measure the deformation of the sealant material is clearly evident in Fig. 2. The sensitivity of the load cells is such that the sealant's mechanical properties for this formulation can be precisely measured in their full range. This is demonstrated by the ability to follow the material from the earliest stages of cure through much later stages of cure. Finally, the error caused by the end play in the jack threads is clearly visible in Fig. 2. After the peak load has been reached in either compression or tension, there is a short section of nonlinear response in the load curves before the load cell data again becomes linear with the deformation step. To account for the end play in screw jacks, the data from the first 0.2 mm of travel in tension is not used in the calculation of the molecular weight between crosslinks.

The calculation of M_c for the four deformation cycles from Fig. 2 is presented in Fig. 3. The 1, 30, and 70 cycle deformation data for a single sample are shown; there is a clear increase in the number of crosslinks shown by a decrease in M_c or increasing slope in these curves. In Fig. 3(b), the data from Fig. 3(a) is plotted in a Mooney-Rivlin format

to check the validity of the use of the neohookean molecular model. In this plot, there is little or no dependence on α. This provides direct evidence that the assumptions invoked in the use of Eq. (1) to link the measured experimental mechanical properties to the molecular model for this set of experiments appears to be a good first approximation.

In Fig. 4, the change in M_c is shown for four samples as a function of cycle number. The calculated values from Fig. 3 are depicted as solid circles. The M_c values show a decrease, which indicates an increase in the number of crosslinks. For values up to 26 cycles, the results all track together, but after this point, each sample begins to deviate.

In Fig. 5, a plot of the maximum tensile stress observed within a deformation cycle is shown. For the first 40 cycles, all of the samples show similar behavior. After 40 cycles, the data for the samples deviate from each other. However, significant adhesion failure was observed in one sample at 30 cycles, which lowers the contact area over which the force is calculated. The total force is now distributed over a smaller now unknown contact area, with two major consequences: first, adhesion failure will progress and second, the reported value for M_c will have additional uncertainty. For example, if half of the sample has debonded, without a significant change in the modulus, it appears in the M_c calculation as a halving of the force or a doubling of the M_c value.

COMPARISON TO THE EXISTING ASTM C719 METHOD

Using the current testing methodology, this particular sealant sample passed ASTM C719 with a ±25% movement classification. The ASTM C719 test specification allows the sealant to pass a series of threshold tests. These involve curing the samples for 21 days, immersion in water for a period of time, storage in a hot oven, and a number of mechanical cycles. At the conclusion of this regime, the samples are judged pass or fail by a visually inspection. By passing this requirement, it is implied that the samples can be used successfully in actual joints that are 0.5 cm and that experience a movement of 25% or less of the joint width.

However, when this sealant was subjected to continuous cyclic movement of 25%, with less than a 21 day cure, all the samples failed in fewer than 90 cycles. While this is a harsh test unlikely to be encountered in actual building environments, it demonstrates the limitations of current sealant certification by ASTM C719 and its derivatives. This device will support the development of a testing method that will quantify the response of a sample to stresses similar to those encountered in the in-service environment. Such tests should lead to better material specifications, installations, and predictions of in-service performance for climatologically local environment.

ACKNOWLEDGMENTS

This project was conducted under the auspices of the NIST Consortium on Service Life Prediction for Sealant that include the Dow Corning, DeGussa, Kanaka Texas, Wacker, SIKA, Tremco, DAP, and Solvay Corporations. The authors are very grateful for the enthusiastic support and fresh insights of these industrial partners. The authors are also grateful for guidance and financial support provided by the Partnership for Advancing Technologies for Housing (PATH) program part of the Policy Development and Research Division of the Department of Housing and Urban Development (HUD). They would like to thank the many colleagues and staff from the Building and Fire Research Laboratory at NIST that have greatly hastened the development of this project.

[1] T. G. B. Jones, A. R. Hutchinson, and A. T. Wolf, Mater. Struct. **34**, 332 (2001).
[2] A. T. Wolf, RILEM Doc SBJ-N002 2001, p. 8.
[3] R. Woolman, *Resealing of Buildings: A Guide to Good Practice* (Butterworth-Heinemann, Oxford, 1995).
[4] R. Chiba *et al.*, *Japan Sealant Industry Association*, Tokyo, Japan, 1992.
[5] E. Grunau, in *Federal Minister for Regional Planning* (Building and Urban Planning, Bonn, Germany, 1976).
[6] National Association of Home Builders, Washington, DC, 2000.
[7] US Census Bureau, Washington DC., 1998.
[8] Materials, A.S.o.T.a., West Conshohokcen, PA, 1998.
[9] L. H. Sperling, *Introduction to Polymer Physical Science*, 2nd ed. (Wiley-Interscience, New York, 1992).
[10] H. E. Adabbo and R. J. J. Williams, J. Appl. Polym. Sci. **27**, 1327 (1982).
[11] A. T. Dibenedetto, J. Polym. Sci., Part B: Polym. Phys. **25**, 1949 (1987).
[12] R. L. Fan *et al.*, J. Appl. Polym. Sci. **81**, 710 (2001).
[13] L. Fang, G. Clausen, and P. O. Fanger, Indoor Air **9**, 193 (1999).
[14] J. K. Gillham, Polym. Int. **44**, 262 (1997).
[15] A. Moradi-Araghi, J. Pet. Sci. Eng. **26**, 1 (2000).
[16] N. Sombatsompop, Polym.-Plast. Technol. Eng. **37**, 333 (1998).
[17] N. Sombatsompop, Cellular Polymers **17**, 63 (1998).
[18] N. Sombatsompop, Polym. Polym. Composites **7**, p. 41 (1999).
[19] R. J. J. Williams and C. C. Riccardi, Macromol. Symp. **93**, 245 (1995).
[20] W. X. Zukas, J. Appl. Polym. Sci. **53**, 429 (1994).
[21] A. R. Payne, Nature (London) **177**, 1174 (1956).
[22] A. N. Gent and P. B. Lindley, Proc. Inst. Mech. Eng. **173**, 111 (1959).
[23] S. A. Ketcham, J. M. Niemiec, and G. B. McKenna, J. Eng. Mech. **669**, 677 (1996).
[24] Identification of a commercial product is made only to facilitate experimental reproducibility and to describe adequately experimental procedure. In no case does it imply endorsement by NIST or imply that it is necessarily the best product for the experiment.
[25] A. T. Wolf, State-of-the-Art Report of the RILEM Technical Committee 139-DBS. Cedex, France: RILEM Publications S.A.R.L., 1999.
[26] V. A. Demerast *et al.*, *ASTM STP 1334* (ASTM, Philadelphia, 1998).